

# Cosmic-Ray Neutron Detectors for Soil Moisture Monitoring

A.M. Dumont<sup>1</sup>, K.D. Moloto<sup>1</sup>, and H. Havenga<sup>2</sup>

<sup>1</sup>Centre for Space Research, North-West University, Potchefstroom 2531, South Africa

<sup>2</sup>Unit for Environmental Sciences and Management, North-West University, Potchefstroom 2531, South Africa

E-mail: [dumont.aimee@gmail.com](mailto:dumont.aimee@gmail.com)

**Abstract.** Primary cosmic-rays are high-energy particles that enter the Earth's atmosphere via the heliosphere, generating cascades of secondary cosmic-ray particles when interacting with atmospheric atoms. These secondary cosmic-rays interact inversely with hydrogen atoms in soil moisture, when measured it provides a non-invasive method for monitoring moisture levels. Continuous neutron flux observations in soil can help to establish predictive models for evaporation, droughts, and floods that significantly impact South Africa's water resources. This study employs a cosmic-ray neutron sensor (CRNS) probe equipped with a Boron trifluoride ( $\text{BF}_3$ ) detector positioned 1-2 m above ground that is capable of measuring soil moisture across a footprint of approximately 20 hectares in width and up to 0.3 m depth. This paper details the calibration process that relates the measured neutron intensity to gravimetric soil sampling. This approach can assist in precision water resource management, especially in a drought prone country such as South Africa.

## 1 Introduction

Agriculture plays a vital role in South-Africa's economy, not only does it add  $\sim 3\%$  to our GDP in 2024, it provides the country with food security and a source of job recreation to  $\sim 1.1$  million people from primary to secondary production [1, 2]. As South Africa has periodic dry spells that affect the agricultural industry, early assessment of soil moisture reserves and constant monitoring could assist with water efficiency and effective crop yield [3, 4, 5, 6].

Primary cosmic-rays collide with atmospheric nuclei, creating cascades of secondary cosmic-ray particles that penetrate the soil, producing fast (epithermal) neutrons [7]. The hydrogen in the soil slows down the epithermal neutrons, creating thermal neutrons [5]. In saturated soils, there will be an abundance of thermal neutrons compared to dry soil. Using this knowledge, Cosmic ray neutron sensing (CRNS), is an accurate and non-invasive method of detecting soil moisture in large areas [8, 9]. This method has been successfully applied in extreme environments in bridging the gap between point sensor data and large scale remote sensing (e.g. satellite) techniques [10, 11]. The sensor measures the background neutron flux, which has an inverse correlation to soil moisture content [12]. This work describes the  $\text{BF}_3$  neutron monitor design and characteristics of the study site with preliminary insights into the relation between neutron count and hydrogen [13].

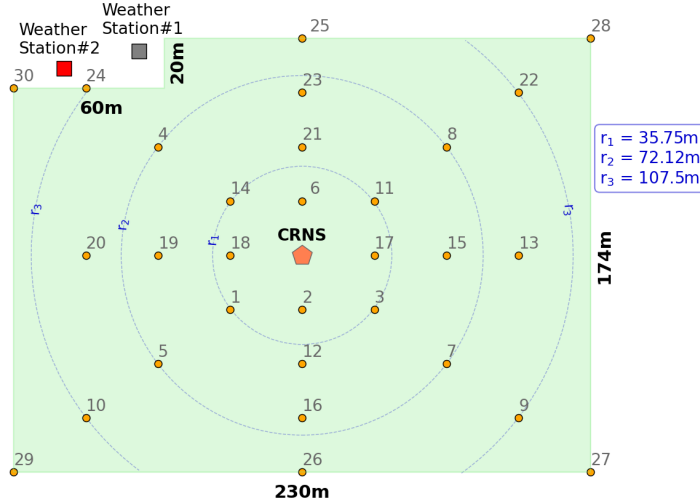


Figure 1: The layout of the site with the locations of instruments. The cosmic-ray neutron sensor (CRNS) is located in the centre of the field, with the soil moisture sensors (represented by orange points) positioned at different radii away from the CRNS. Two weather stations are positioned next to the field, as well as lead and lead-free neutron monitors (NM) are located in the shed for calibrating the CRNS.

## 2 Site description

Pienaarsskamp farm is part of the North-West University (NWU) Center for Sustainable Agriculture and is located  $\sim 5$  km from the Potchefstroom campus in North-West, South Africa ( $S26^{\circ}38'59.99''$ ,  $E27^{\circ}5'23.99''$ ). This study focuses on a field at the Pienaarsskamp farm that covers an area of  $\sim 3.88$  hectares. The soil is classified as a Magudu soil formation, the soil contains between 10 – 20% of clay and appears to be reddish in colour on the structured horizon and a yellow-brown colour on the apedal horizon [14]. The site is located on slightly heterogeneous terrain, where the soil freely drains water, which is mainly used for agricultural purposes, and is fenced off to prevent cattle grazing. During various phases of this project Sunflowers were planted and harvested on the selected field.

The CRNS (which is a lead-free neutron monitor) is located at the centre of the field, as seen in Figure 1, and is surrounded by 30 soil moisture sensors. The shed is located  $\sim 100$  m away from the field, which harbours the lead neutron monitor and the lead-free neutron monitor.

## 3 Neutron monitor design



Figure 2: (a) Lead neutron monitor (b) Lead-free neutron monitor (c) Detailed front view of the lead neutron monitor

Three neutron monitors (as seen in Figure 2) were installed on the NWU Pienaarsskamp. Two of the neutron monitors are located in a shed, on a solid concrete platform (shown in Figure 2 (a) and Figure 2 (b)), and one

neutron monitor is located in the centre of the field described earlier (shown in Figure 3 (c)). The following subsections discusses the physical aspects and detection processes of the neutron monitors, which are detailed below.

### 3.1 Physical design

One of the neutron monitors in the shed is the lead neutron monitor (shown in Figure 2 (a)) that consists of a gas-filled detector surrounded by a thin inner polyethylene cylinder; this is placed inside the seven lead rings which are then encased in a thick outer polyethylene cylinder (as shown in Figure 2 (c)). The other neutron monitor (Figure 2(b)) is the lead-free neutron monitor (also referred to as the "bare" neutron monitor) that consists of a gas-filled detector encased in a polyethylene moderator cylinder (which is the same as the inner polyethylene cylinder in the lead neutron monitor). The neutron monitor positioned in the field (Figure 3(c)) is a lead-free neutron monitor, except that it is placed vertically, unlike the other neutron monitors, which are placed horizontally. Here, the gas-filled detectors, shielding, and the lead around the detector are discussed in detail.

Type	Efficiency	Cost	Long term
$\text{BF}_3$	Less efficient	Inexpensive	Stable over long periods, can decrease from deposition on the anode wire
$^3\text{He}$	More efficient	Expensive	Shows drift parameters after a period due to helium leakage

Table 1: Comparison between the  $\text{BF}_3$  and  $^3\text{He}$  gas in neutron monitors [15].

#### 3.1.1 Gas-filled thermal-neutron detectors

Gas-filled detectors are used to detect thermal neutrons (neutrons with  $\sim 0.025$  eV) as atmospheric neutron particles react with the gas [16, 12]. There are two main gas-filled thermal neutron detectors, Helium-3 ( $^3\text{He}$ ) and Boron Trifluoride ( $\text{BF}_3$ ), where both produce exothermic reactions and have strong neutron absorption cross-section [17, 18].  $^3\text{He}$  is not commonly used even though it performs similarly to  $\text{BF}_3$  in standard neutron monitors; there are a few differences between the gases that are summarised in Table 1 [16, 15]. The gas-filled thermal neutron detectors used in this study are  $\text{BF}_3$  LND20366<sup>1</sup> tubes, which are stable over long periods. These neutron detectors are stainless steel tubes with diameters of 51 mm and lengths of 652 mm. When high voltage is transmitted through the  $\text{BF}_3$  molecules and ionises the gas, creating a  $(n, \alpha)$  that splits the  $\text{BF}_3$  molecules into alpha particles and lithium nuclei; this creates absorption of atmospheric neutron particles through the walls of the LND20366 tube.[17, 19, 20]. Having a gas-filled tube creates leakage of thermal neutrons and is susceptible to background radiation; therefore, the thin polyethylene cylinder decreases the amount of thermal neutrons and the background sensitivity by 30% while increasing the efficiency of neutron flux detected [20].

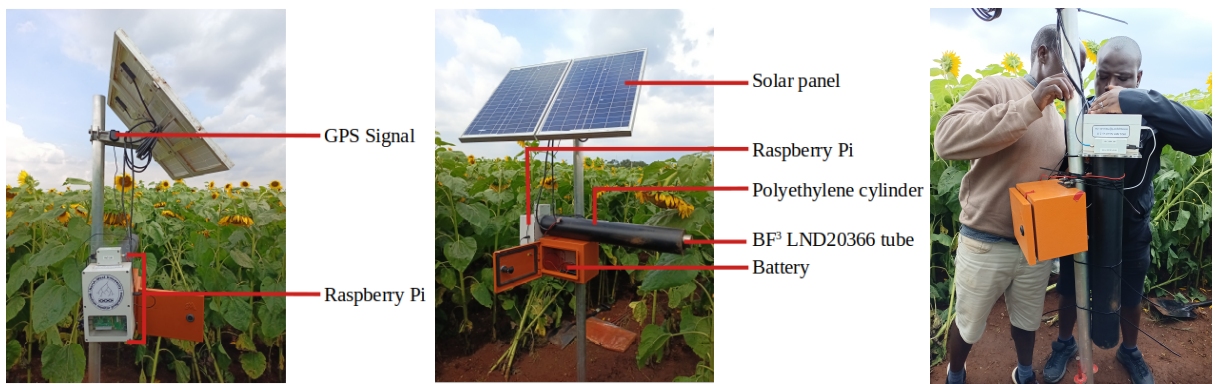


Figure 3: Components of the field NM. (a) Detailed front view of the field NM. (b) Detailed side view of the field nm. (c) Final position of the field NM, to decrease background neutron sensitivity.

<sup>1</sup>gas-filled tubes are manufactured by LND Inc., USA and are available through <https://www.lndinc.com/>.

### 3.1.2 Lead and Shielding around the detector

There are seven lead rings inside the external polyethylene cylinder (as shown in Figure 2 (c)), each lead ring weighs  $\sim 25$  kg. The lead has a higher atomic mass, which creates secondary neutron particles (neutrons that are produced through the interaction with the  $\text{BF}_3$  gas) through non-elastic interactions in which the lead nuclei become excited [21, 22]. This increases the detection of epithermal neutrons (neutrons that have an energy  $\geq 0.5$  eV) as the lead can produce multiple neutrons from a single atmospheric cosmic ray [12, 23]. The thick outer polyethylene cylinder of the lead neutron monitors shields the neutron monitor from detecting background radiation while containing the neutrons that were produced from the lead rings [24].

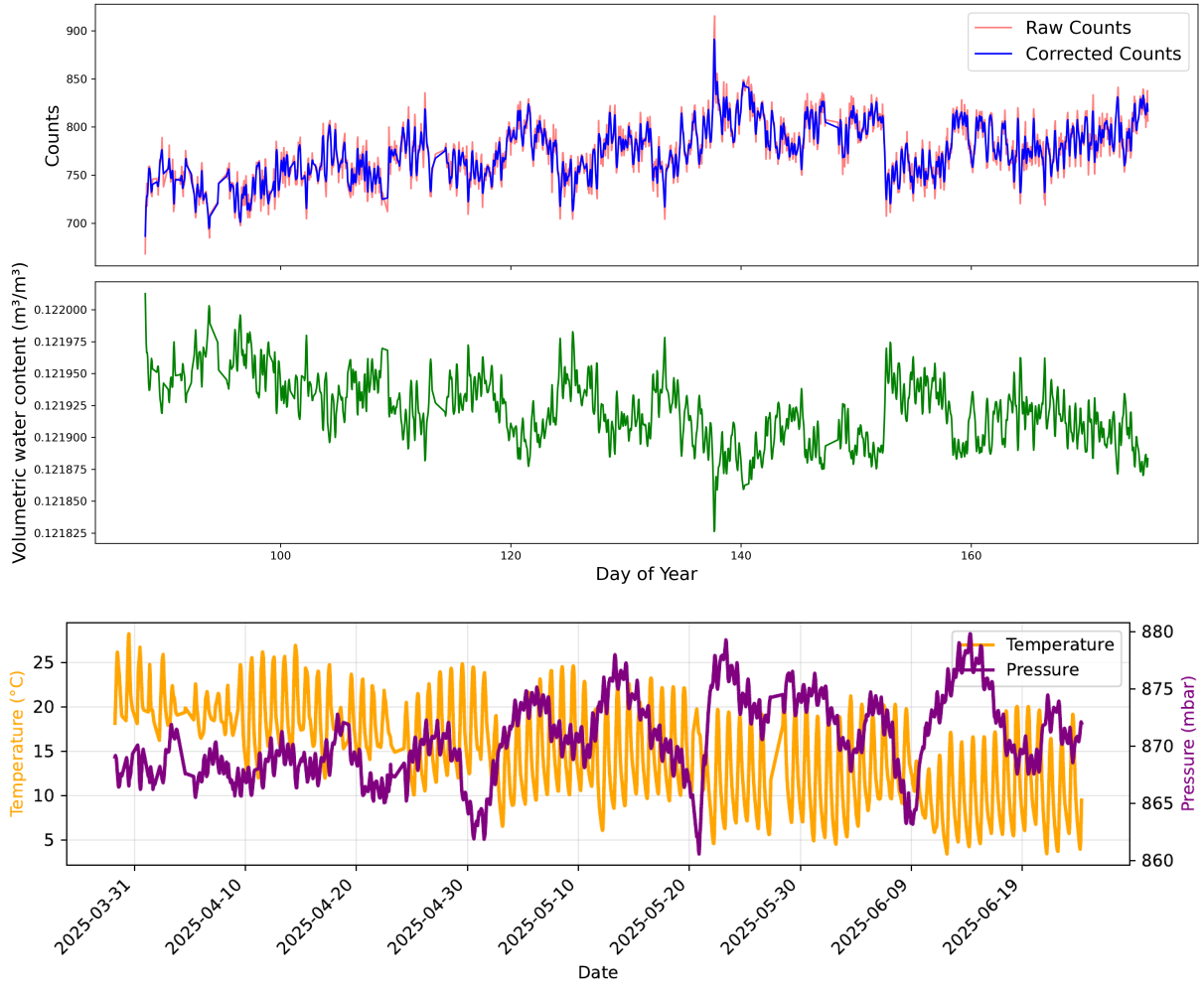


Figure 4: The first panel shows the raw count rates and the corrected count rates of the lead-free neutron monitor, which was obtained hourly between 27 March 2025 – 24th June 2025. The second panel shows the percentage of volumetric water content from the neutron flux. The third panel shows the temperature and pressure.

### 3.2 Electronic components

Figure 3 shows all the electronics in the neutron monitors as detailed by Strauss et al. [15], where the head of the LND20366 tube is connected to the Raspberry Pi data logger, which was manufactured at the NWU. The solar panel is the power supply for the field neutron monitor, which transmits high voltage through the LND20366 tube and the data logger; the neutron monitors in the shed use a standard 230 V plug outlet. The GPS signal is used to ensure that the Raspberry Pi has the location and time to catalogue data. The system uses a 5V output solar-powered battery; during deployment, it was realised that the battery used was not sufficient to supply the system during initial startup, which led to invalid data on the field sensor. The data logger contains Python 3 scripts to

catalogue the raw count rate data, temperature, pressure, and the high voltage transmitted through the gas. The raw data then gets binned in minute intervals when the scripts are processed in the Raspberry Pi.

#### 4 Neutron count rate processing

Desilets et al. [25] determined that the conversion of count rates to volumetric water content ( $\Theta(N)$ ) equation is given by,

$$\Theta(N) = \frac{a_0}{\left(\frac{N}{N_0}\right) - a_1} - a_2 ; \quad (1)$$

where,

$$a_0 = 0.0808, \quad a_1 = 0.372, \quad a_2 = 0.0115 . \quad (2)$$

Here  $a_0$ ,  $a_1$ , and  $a_2$  are empirical parameters of near-surface neutron intensity of a generic silica soil matrix,  $N$  is the corrected neutron count rate, and  $N_0$  is the neutron count rate over dry soil [25, 26]. Köhli et al. [13] simplified Equation 1 and can be expressed as,

$$\Theta(N) = \tilde{a}_0 \left( \frac{1 - N/N_{max}}{\tilde{a}_1 - N/N_{max}} \right) \quad (3)$$

where,

$$\tilde{a}_0 = -a_2, \quad \tilde{a}_1 = \frac{a_1 a - 2}{a_0 + a_1 a_2}, \quad N_{max} = \frac{a_0 + a_1 a_2}{a_2 N_0} . \quad (4)$$

#### 5 Preliminary results

The first panel in Figure 4 represents the hourly neutron count rate for the lead-free neutron monitor. This neutron monitor was installed at Pienaarskamp farm on the 27th March 2025, and is placed horizontally over a solid concrete platform. The second panel in Figure 4 converts the neutron count rates of the lead-free monitor to volumetric water content using Equation 1 where  $N$  is the lead-free count rates and  $N_0$  are the lead count rates. Although the second panel does not show much of an increase in volumetric water content, these readings can still be used to identify rainfall. An inverse correlation between the volumetric water and the count rate can be observed between the first two panels. The last panel shows the temperature and pressure from the lead-free neutron monitor, where an inverse correlation between the two can be observed. The temperature can be seen decreasing over time; this is due to seasonal changes from summer to winter.

#### 6 Conclusion

This paper presents the calibration process of a CRNS setup, even though the field neutron monitor data was unattainable, the process was conducted via the neutron monitors in the shed. The results showed that the neutron monitors could sense excess hydrogen atoms in the atmosphere.

In addition to future calibrations of the CRNS, the voltage of the Field neutron monitor would have to be increased to obtain viable data, this highlights some limitations of calibration during field deployments such as we attempted here. In addition, the volumetric water content should be compared to the data obtained from the soil sensors. Furthermore, the volumetric and volumetric water content should be modelled to the rainfall in the area to distinguish if this is an accurate and efficient method for determining the amount of moisture in the soil. However, the potential to use this technology in operational settings for water management remains promising and further investigations are being conducted to improve the instrument design, calibration of soil moisture to neutron flux using point sensors, and the application in real-world scenarios.

#### References

- [1] Mar 2025. [Online]. Available: <https://www.gov.za/blog/agriculture-vital-part-our-growth-story>
- [2] Mar 2025. [Online]. Available: <https://nda.gov.za/images/Branches/EconomicDevelopmentTradeandMarketing/StatisticaandEconomicAnalysis/statistical-information/economic-review-of-the-south-african-agriculture-2024.pdf>
- [3] A. Bennie and M. Hensley, “Advances in soil physics and soil water management research in south africa, 1979–2003,” *South African Journal of Plant and Soil*, vol. 21, no. 5, pp. 268–277, 2004.
- [4] H. McNairn, A. Merzouki, A. Pacheco, and J. Fitzmaurice, “Monitoring soil moisture to support risk reduction for the agriculture sector using radarsat-2,” *IEEE Journal of Selected Topics in Applied Earth Observations and Remote Sensing*, vol. 5, no. 3, pp. 824–834, 2012.

[5] E. van Amelrooij, N. van de Giesen, J. Plomp, M. Thijs, and T. Fico, “Blosm: Boron-based large-scale observation of soil moisture: First laboratory results of a cost-efficient neutron detector,” *HardwareX*, vol. 12, p. e00342, 2022.

[6] K. Furtak and A. Wolińska, “The impact of extreme weather events as a consequence of climate change on the soil moisture and on the quality of the soil environment and agriculture—a review,” *Catena*, vol. 231, p. 107378, 2023.

[7] M. Zreda, D. Desilets, T. Ferré, and R. L. Scott, “Measuring soil moisture content non-invasively at intermediate spatial scale using cosmic-ray neutrons,” *Geophysical research letters*, vol. 35, no. 21, 2008.

[8] A. Hawdon, D. McJannet, and J. Wallace, “Calibration and correction procedures for cosmic-ray neutron soil moisture probes located across australia,” *Water Resources Research*, vol. 50, no. 6, pp. 5029–5043, 2014.

[9] J. Jakobi, J. A. Huisman, H. Fuchs, H. Vereecken, and H. Bogena, “Potential of thermal neutrons to correct cosmic-ray neutron soil moisture content measurements for dynamic biomass effects,” *Water resources research*, vol. 58, no. 8, p. e2022WR031972, 2022.

[10] L. M. Scheiffele, G. Baroni, T. E. Franz, J. Jakobi, and S. E. Oswald, “A profile shape correction to reduce the vertical sensitivity of cosmic-ray neutron sensing of soil moisture,” *Vadose Zone Journal*, vol. 19, no. 1, p. e20083, 2020.

[11] L. Myeni, M. E. Moeletsi, and A. D. Clulow, “Development and analysis of a long-term soil moisture data set in three different agroclimatic zones of south africa,” *South African Journal of Science*, vol. 117, no. 5-6, 2021.

[12] M. Zreda, W. Shuttleworth, X. Zeng, C. Zweck, D. Desilets, T. Franz, and R. Rosolem, “Cosmos: The cosmic-ray soil moisture observing system,” *Hydrology and Earth System Sciences*, vol. 16, no. 11, pp. 4079–4099, 2012.

[13] M. Köhli, J. Weimar, M. Schrön, R. Baatz, and U. Schmidt, “Soil moisture and air humidity dependence of the above-ground cosmic-ray neutron intensity,” *Frontiers in Water*, vol. 2, p. 544847, 2021.

[14] S. C. W. Group, *Soil classification: a taxonomic system for South Africa*. Department of Agricultural Development, 1991, vol. 15.

[15] D. T. Strauss, S. Poluianov, C. Van Der Merwe, H. Krüger, C. Diedericks, H. Krüger, I. Ussoskin, B. Heber, R. Nndanganeni, J. Blanco-Ávalos *et al.*, “The mini-neutron monitor: a new approach in neutron monitor design,” *Journal of space weather and space climate*, vol. 10, p. 39, 2020.

[16] P. H. Stoker, L. I. Dorman, and J. M. Clem, “Neutron monitor design improvements,” *Space Science Reviews*, vol. 93, no. 1, pp. 361–380, 2000.

[17] T. Crane and M. Baker, “Neutron detectors,” *Passive Nondestructive Assay of Nuclear Materials*, vol. 13, pp. 1–28, 1991.

[18] P. Chatzispyroglou, J. L. Keddie, and P. J. Sellin, “Boron-loaded polymeric sensor for the direct detection of thermal neutrons,” *ACS Applied Materials & Interfaces*, vol. 12, no. 29, pp. 33 050–33 057, 2020.

[19] W. Abson, P. Salmon, and S. Pyrah, “Neutron counters,” *Journal of the Institution of Electrical Engineers*, vol. 4, no. 41, pp. 252–255, 1958.

[20] G. Grosshoeg, “Neutron ionization chambers,” *Nuclear instruments and Methods*, vol. 162, no. 1-3, pp. 125–160, 1979.

[21] Y. V. Balabin, B. Gvozdevsk, E. Maurchev, E. Vashenyuk, and D. Dzhappuev, “Fine structure of neutron multiplicity on neutron monitors,” *Astrophysics and Space Sciences Transactions (ASTRA)*, vol. 7, no. 3, p. 283, 2011.

[22] R. Bütkofer, “Ground-based measurements of energetic particles by neutron monitors,” *Solar particle radiation storms forecasting and analysis*, vol. 444, pp. 95–112, 2018.

[23] N. Aiemsad, D. Ruffolo, A. Sáiz, P.-S. Mangeard, T. Nutaro, W. Nuntiyakul, N. Kamyan, T. Khumlumlert, H. Krüger, H. Moraal *et al.*, “Measurement and simulation of neutron monitor count rate dependence on surrounding structure,” *Journal of Geophysical Research: Space Physics*, vol. 120, no. 7, pp. 5253–5265, 2015.

- [24] W. Nuntiyakul, A. Sáiz, D. Ruffolo, P.-S. Mangeard, P. Evenson, J. Bieber, J. Clem, R. Pyle, M. Duldig, and J. Humble, “Bare neutron counter and neutron monitor response to cosmic rays during a 1995 latitude survey,” *Journal of Geophysical Research: Space Physics*, vol. 123, no. 9, pp. 7181–7195, 2018.
- [25] D. Desilets, M. Zreda, and T. P. Ferré, “Nature’s neutron probe: Land surface hydrology at an elusive scale with cosmic rays,” *Water Resources Research*, vol. 46, no. 11, 2010.
- [26] L. Stevanato, G. Baroni, Y. Cohen, C. L. Fontana, S. Gatto, M. Lunardon, F. Marinello, S. Moretto, and L. Morselli, “A novel cosmic-ray neutron sensor for soil moisture estimation over large areas,” *Agriculture*, vol. 9, no. 9, p. 202, 2019.